ANALYSIS OF FLUORESCENCE DECAY BY THE NONLINEAR LEAST SQUARES METHOD

N. PERIASAMY
Chemical Physics Group, Tata Institute of Fundamental Research, Homi Bhabha Road, Colaba, Bombay : 400 005, India

ABSTRACT Fluorescence decay deconvolution analysis to fit a multiexponential function by the nonlinear least squares method requires numerical calculation of a convolution integral. A linear approximation of the successive data of the instrument response function is proposed for the computation of the convolution integral. Deconvolution analysis of simulated fluorescence data were carried out to show that the linear approximation method is generally better when one of the lifetimes is comparable to the time interval between data.

INTRODUCTION

Time-resolved fluorescence decay measurements provide important information about the structure and dynamics of the system under investigation. In a general application the experimental fluorescence decay data is fitted to a decay function, $I(t)$, which is derived for an assumed model. Nonlinear least squares method (1, 2) is generally used in fitting the data to the function $I(t)$ and one obtains optimum values for the adjustable parameters in $I(t)$. This method requires numerical evaluation of the convolution integral (Eq. [1]) and the partial derivatives of $F(t)$ with respect to the adjustable parameters. $R(t)$ in Eq. (1) is the instrument response function or excitation function.

$$F(t) = \int_0^t R(s)\, I(t - s)\, ds. \tag{1}$$

When $I(t)$ is a multiexponential function, $\Sigma_i A_i \exp(-t/\tau_i)$, A_i, and τ_i are the adjustable parameters. Grinvald and Steinberg (3) proposed an algorithm based on the trapezoidal approximation for the numerical integration. This method is widely used, though other approximations (Simpson's rule and law of the mean) are also found to be equally good (4). In these approximations it is implicitly assumed that the excitation function is a series of delta functions separated in time. However, the pulsed light sources employed in experiments are expected to have a continuous variation of intensity with time and hence the excitation function used in deconvolution ought to be continuous. Here, we construct a continuous excitation function using the discrete excitation data by assuming a linear variation between the discrete data. Numerical calculation of $F(t)$ can then be carried out using integrated expressions. The performance of this new method to calculate $F(t)$ is compared with that of Grinvald-Steinberg method in the analysis of fluorescence data simulated under various conditions.

MATHEMATICAL EQUATIONS

Consider that $R_1, \ldots R_i, \ldots R_n$ are the n numerical data of the instrument response function and δt is the time interval between R_i and R_{i-1}. In the linear approximation $R(t)$ is considered as $(n-1)$ step functions $(R_1[t], R_2[t], \ldots R_j[t] \ldots R_{n-1}[t])$ represented by Eq. (2).

$$R_j(t) = m_j t + c_j, \text{ for } j < t \le (j+1)\delta t$$
$$= 0, \quad \text{otherwise} \tag{2}$$

m_j and c_j are the slope and intercept of the line joining R_i and R_{i-1}. The convolution integral (Eq. [1]) can then be written as,

$$F_i = \sum_{j=1}^{i-1} \int_{(j-1)\delta t}^{j\delta t} R_j(s)\, I[(i-1)\delta t - s]\, ds \tag{3}$$

for $i \neq 1$. When $I(t)$ is a sum of p exponentials,

$$I(t) = \sum_{k=1}^{p} A_k \exp(-t/\tau_k). \tag{4}$$

Eq. (3) is integrated to give the following recursion relation:

$$F_i^k = F_{i-1}^k \exp(-\delta t/\tau_k) + A_k\tau_k \{R_i - R_{i-1} \exp(-\delta t/\tau_k) - m_{i-1}\tau_k [1 - \exp(-\delta t/\tau_k)]\} \tag{5}$$

$$F_i = \sum_{k=1}^{p} F_i^k. \tag{6}$$

The partial derivatives of $F(t)$ are given by Eqs. (7) and (8) summed over all k.

$$(\partial F_i^k/\partial A_k) = (F_i^k/A) \tag{7}$$

$$(\partial F_i^k/\partial \tau_k) = \exp(-\delta t/\tau_k)[(\partial F_{i-1}^k/\partial \tau_k) + F_{i-1}^k(\delta t/\tau_k^2)] + A[R_i - R_{i-1}\exp(-\delta t/\tau_k)\{1 + (\delta t/\tau_k)\} - 2\, m_{i-1}\tau_k\{1 - \exp(-\delta t/\tau_k)\} + m_{i-1}\,\delta t \exp(-\delta t/\tau_k)]. \quad (8)$$

For $i = 1$, $F_1^k \simeq A_k\,\delta t\,R_1$, $(\partial F_1^k/\partial A_k) \simeq \delta t\,R_1$ and $(\partial F_1^k/\partial \tau_k) = 0$. When $R_1 = 0$, which condition is usually met in experiments, F_1^k and its derivatives are zero.

It is noted that for $\tau_k \gg \delta t$

$$F_i^k = F_{i-1}^k \exp(-\delta t/\tau_k) + 0.5\,(R_{i-1} + R_i)A\,\delta t \quad (9)$$

and

$$(\partial F_i^k/\partial \tau_k) = (\partial F_{i-1}^k/\partial \tau_k)\exp(-\delta t/\tau_k), \quad (10)$$

which agree closely with the Grinvald-Steinberg equations. However, for $\tau_k \lesssim \delta t$ Eqs. (5) and (8) give results which are substantially different from the Grinvald-Steinberg equations. Thus use of Eqs. (5), (7), and (8) is expected to yield quantitatively different results when τ_k is comparable with δt. This expectation is tested using simulated fluorescence decay data, the details of which are described below.

SIMULATION OF DATA AND ANALYSIS

The deconvolution algorithm using Eqs. (5), (7), and (8) is denoted as method I and the algorithm using the Grinvald-Steinberg equations is denoted as method II. The deconvolution algorithm for both the methods is identical in all other aspects. The performances of both the methods were tested by using simulated fluorescence decay data.

Four different functions for $R(t)$ were chosen for the purpose of simulating fluorescence data. These functions are given by Eqs. (11)–(14).

$$R(t) = W\exp[-(t - m)^2/2\sigma^2] \quad (11)$$

$$R(t) = W[\exp(-t/\alpha) - \exp(-t/\beta)] \quad (12)$$

$$R(t) = W\,t^2\exp(-t/\gamma) \quad (13)$$

$$R(t) = W[t^2\exp(-t/\gamma) + 10^{-3}\,t\exp(-t/\epsilon)]. \quad (14)$$

W is the scaling constant in the above equations. m, σ, α, β, γ, and ϵ are all constants. Eq. (11) gives a symmetric Gaussian profile for the excitation function. Eq. (12) or (13) gives an asymmetric profile for the excitation function. Eq. (14) gives an asymmetric profile with a long tail determined by the value of ϵ ($> \gamma$). Such long tails are common in experiments using flash lamps. For the above excitation functions the rise time and pulse width are adjustable by varying m and σ (Eq. 11), α and β (Eq. 12) and γ (Eqs. 13 and 14). The values of m, σ (Eq. 11), α, β (Eq. 12), and γ (Eqs. 13 and 14) were chosen to produce excitation pulse with a full-width at half-maximum varying from 0.40 ns (8 channels) to 4 ns (80 channels). For each excitation function, excitation data R_i were calculated in the interval of 50 ps and the data was normalised for a peak value of 1×10^5.

The fluorescence decay function $I(t)$ was chosen to be a double exponential function (Eq. 15):

$$I(t) = A_1\exp(-t/\tau_1) + A_2\exp(-t/\tau_2), \quad (15)$$

where A_1, τ_1, A_2, and τ_2 are the parameters optimised in the deconvolution analysis. Simulation of emission data and analysis by methods I and II can be done for any choice of A_1, τ_1, A_2, and τ_2. It will be shown later that methods I and II perform equally well when $\tau_1 \gg \delta t$, and $\tau_2 \gg \delta t$, which is expected from the mathematical equations. Hence, emphasis was given to the variation of the short lifetime component: the amplitude and lifetime. The following values for the parameters were used in the simulation of data: $A_1 = 10$ or 1, $\tau_1 = 0.02, 0.05, 0.1$ or 0.2 ns, $A_2 = 1$ and $\tau_2 = 2$ ns.

Simulation of the fluorescence data F_i is done by the evaluation of the integral in Eq. (1). In the case of Eq. (11) for $R(t)$ the integral was evaluated numerically (sum rule) at an interval of 0.5 ps and then selecting data in 50 ps interval. In the case of Eqs. (12), (13), or (14), Eq. (1) was integrable and the fluorescence data was calculated from the analytic equation for $F(t)$. After the computation of 512 data for F_i, the fluorescence data is normalised for a peak value of 1×10^5. This normalisation alters the value of A_1 and A_2 but the ratio (A_1/A_2) remains unchanged.

The data of R_i obtained from Eqs. (11)–(14) and the fluorescence emission data F_i evaluated using Eq. (1) are noise-free. Gaussian noise is then added to R_i and F_i, so that the noise-added data resembles experimental data obtained in time-correlated single photon counting experiments. It is well known (5) that for F_i (or R_i) > 20, the Gaussian noise is approximately equal to the Poisson noise encountered in photon counting experiments. The Gaussian noise for the 512 data of excitation or emission function is computed (5) using a sequence of pseudo-random numbers which are generated using a seed. The seed itself is a random number. This method ensures that (*a*) the pattern of noise in the excitation data is different from that of the emission data, and (*b*) no two patterns of noise used in the hundreds of simulations are identical.

The deconvolution analysis of fluorescence decay data by the nonlinear least-squares method using Marquardt procedure requires starting values for the parameters A_1, τ_1, A_2, and τ_2. Several iterations are usually required by methods I and II for the completion of analysis which is determined by the criterion that successive iterations do not change the optimised value of each of the four parameters by more than 1 in 10^6. The results of the analysis by either method are independent of the starting values of A_1, τ_1, A_2, and τ_2. The set of values (4.0, 0.8, 2.0, 0.2) has been uniformly used as the starting values for $(A_1, \tau_1, A_2, \tau_2)$. In a few sets of data, analysis by method I or method II or by both the methods led to optimised values far from expected

ones with chi-square $\gg 1$, which indicated convergence to a local minimum in the chi-square hypersurface. In such cases another set of starting values for $(A_1, \tau_1, A_2, \tau_2)$ was used for successful analysis.

After completion of the analysis, optimised values for A_1, τ_1, A_2, and τ_2 are obtained. The goodness of fit is usually determined by the randomness of the weighted residuals. Several statistical tests are routinely carried out to check the randomness of the weighted residuals, the calculation of reduced chi-square (CHISQ) being the most important one. The other statistical test parameters calculated are (4, 6) (*a*) Durbin-Watson parameter (DWP) (*b*) Standard normal variate of ordinary runs test (Z) and (*c*) percentage of weighted residuals in the range of -2 to $+2$ (PER).

The simulation of data using Eqs. (11)–(14) for R_i and Eq. (15) for F_i was carried out in the following manner: For each $R(t)$ three excitation functions of varying pulsewidth were generated. These excitation functions are labeled A, B, C for Eq. (11), D, E, F for Eq. (12), G, H, I for Eq. (13), and J, K, L for Eq. (14). The pulsewidths and the values of parameters of the excitation functions A to L are given in Tables I to IV. As mentioned earlier eight combinations of $(A_1, \tau_1, A_2, \tau_2)$ were used in the decay Eq. $I(t)$ for the simulation of emission data. The long-lifetime parameters A_2 and τ_2 were held constant in all. The values of the eight sets are given in Table I for the excitation function A. For each excitation function and decay function, ten simulations were carried out in which the noise pattern alone was different. Thus, 960 ($8 \times 12 \times 10$) sets of excitation and emission data were simulated and the results of the analysis by methods I and II are given below.

The optimised value of τ_2 by both the methods was in excellent agreement with the expected value of 2.0 ns in all 960 data analysis. However, the optimised values of (A_1/A_2) and τ_1 obtained by method I were significantly different from those obtained by method II. These results are given in Tables I to IV along with the reduced chi-square values obtained by both the methods. For the sake of compactness values of other statistical test parameters are not given in the Tables. However, the values of the other statistical test parameters were generally in agreement with the chi-square criterion. Column 1 in the Tables gives the values for $(A_1, \tau_1, A_2, \tau_2)$. Columns 2, 4, and 6 give the average and standard deviation of the ten optimised values of (A_1/A_2), τ_1, and CHISQ, respectively, obtained by method I. The values given in columns 3, 5, and 7 are those obtained by method II. In each Table complete results are given for one excitation function only. The trend of the results is similar for the other two excitation functions also and hence only partial results are given.

It is seen in Table I (lines 1–8 for excitation function A) that the optimised values of (A_1/A_2) and τ_1 obtained by method I are in better agreement with the expected values than those obtained by method II. In addition, the value of CHISQ obtained by method I is closer to unity than those obtained by method II. In the case of $(A_1, \tau_1, A_2, \tau_2) = (10, 0.02, 1, 2)$ it is noticed that the optimised values of (A_1/A_2)

TABLE I
RESULTS OF ANALYSIS BY METHODS I AND II OF DATA SIMULATED USING
$R(t) = W \exp[-(t-m)^2/2\sigma^2]$

	(A_1/A_2)*		τ_1*		CHISQ*	
	I	II	I	II	I	II
A $\sigma = 0.2$ ns; $m = 1.2$ ns; FWHM = 0.40 ns						
10,2,1,2	10.0 ± 0.02	9.86 ± 0.02	0.200 ± 0.001	0.202 ± 0.001	1.16 ± 0.13	1.28 ± 0.14
1,0.2,1,2	0.99 ± 0.01	0.97 ± 0.01	0.203 ± 0.002	0.207 ± 0.002	1.12 ± 0.07	1.15 ± 0.06
10,0.1,1,2	9.96 ± 0.03	9.38 ± 0.03	0.101 ± 0.001	0.105 ± 0.001	1.13 ± 0.14	1.32 ± 0.17
1,0.1,1,2	0.97 ± 0.02	0.90 ± 0.01	0.104 ± 0.002	0.110 ± 0.002	1.12 ± 0.16	1.15 ± 0.17
10,0.05,1,2	9.87 ± 0.07	8.12 ± 0.04	0.051 ± ‡	0.058 ± ‡	1.14 ± 0.12	1.27 ± 0.14
1,0.05,1,2	0.89 ± 0.03	0.74 ± 0.02	0.057 ± 0.002	0.065 ± 0.002	1.05 ± 0.098	1.06 ± 0.10
10,0.02,1,2	9.50 ± 0.26	5.27 ± 0.05	0.021 ± 0.001	0.032 ± 0.001	1.07 ± 0.09	1.10 ± 0.09
1,0.02,1,2	0.58 ± 0.09	0.41 ± 0.04	0.037 ± 0.006	0.047 ± 0.006	1.05 ± 0.09	1.05 ± 0.09
B $\sigma = 0.5$ ns; $m = 2.5$ ns; FWHM = 1.00 ns						
10,0.1,1,2	9.94 ± 0.08	9.35 ± 0.07	0.101 ± 0.001	0.105 ± 0.001	1.05 ± 0.09	1.04 ± 0.08
1,0.02,1,2	0.66 ± 0.29	0.43 ± 0.12	0.035 ± 0.012	0.043 ± 0.013	1.05 ± 0.11	1.04 ± 0.11
C $\sigma = 0.75$ ns; $m = 3.5$ ns; FWHM = 1.75 ns						
10,0.1,1,2	10.08 ± 0.12	9.46 ± 0.10	0.099 ± 0.001	0.104 ± 0.001	1.10 ± 0.11	1.10 ± 0.11
1,0.02,1,2	0.77 ± 0.46	0.50 ± 0.21	0.40 ± 0.027	0.041 ± 0.032	1.04 ± 0.07	1.04 ± 0.07

*Average and standard deviation of ten optimised values for each $(A_1, \tau_1, A_2, \tau_2)$.
‡τ_1 and τ_2 values are in nanoseconds.
§Standard deviation is <0.0005.

TABLE II

RESULTS OF ANALYSIS BY METHODS I AND II OF DATA SIMULATED USING $R(t) = W(e^{-t/\alpha} - e^{-t/\beta})$

	(A_1/A_2)*		τ_1*		CHISQ*	
	I	II	I	II	I	II
D α = 0.5 ns; β = 0.25 ns; FWHM = 0.9 ns						
10,0.2,1,2	10.07 ± 0.03	9.90 ± 0.03	0.198 ± 0.001	0.201 ± 0.001	1.05 ± 0.13	1.06 ± 0.15
1,0.2,1,2	1.03 ± 0.01	1.00 ± 0.01	0.195 ± 0.002	0.200 ± 0.002	1.12 ± 0.07	1.10 ± 0.06
10,0.1,1,2	10.21 ± 0.05	9.48 ± 0.05	0.098 ± 0.001	0.104 ± 0.001	1.12 ± 0.08	1.15 ± 0.07
1,0.1,1.2	1.05 ± 0.02	0.96 ± 0.02	0.096 ± 0.002	0.104 ± 0.002	1.07 ± 0.07	1.06 ± 0.08
10,0.05,1,2	10.40 ± 0.14	8.23 ± 0.07	0.048 ± 0.001	0.058 ± 0.001	1.09 ± 0.16	1.19 ± 0.14
1,0.05,1,2	1.13 ± 0.06	0.86 ± 0.03	0.045 ± 0.003	0.056 ± 0.002	1.03 ± 0.06	1.03 ± 0.07
10,0.02,1,2	10.85 ± 0.30	5.42 ± 0.05	0.018 ± 0.001	0.031 ± 0.001	1.02 ± 0.04	1.05 ± 0.03
1,0.02,1,2	1.27 ± 0.19	0.58 ± 0.03	0.017 ± 0.003	0.030 ± 0.003	1.01 ± 0.14	1.01 ± 0.14
E α = 1.0 ns; β = 0.5 ns; FWHM = 1.75 ns						
10,0.1,1,2	10.10 ± 0.08	9.39 ± 0.06	0.099 ± 0.001	0.105 ± 0.001	1.16 ± 0.28	1.22 ± 0.29
1,0.02,1,2	1.40 ± 0.06	0.57 ± 0.06	0.017 ± 0.006	0.029 ± 0.006	1.09 ± 0.13	1.09 ± 0.13
F α = 2.5 ns; β = 1.0 ns; FWHM = 4.0 ns						
10,0.1,1,2	10.03 ± 0.09	9.33 ± 0.07	0.100 ± 0.001	0.106 ± 0.001	1.03 ± 0.05	1.05 ± 0.05
1,0.02,1,2	0.90 ± 0.22	0.54 ± 0.05	0.24 ± 0.005	0.031 ± 0.005	0.98 ± 0.04	0.98 ± 0.04

*Average and standard deviation of ten values.
‡τ_1 and τ_2 are in nanoseconds.

TABLE III

RESULTS OF ANALYSIS BY METHODS I AND II OF DATA SIMULATED USING $R(t) = Wt^2e^{-t/\gamma}$

	(A_1/A_2)*		τ_1*		CHISQ*	
	I	II	I	II	I	II
G γ = 0.2 ns; FWHM = 0.65 ns						
10,0.2,1,2	9.98 ± 0.04	9.82 ± 0.04	0.201 ± 0.001	0.204 ± 0.001	1.53 ± 0.15	1.86 ± 0.15
1,0.2,1,2	0.99 ± 0.01	0.96 ± 0.01	0.203 ± 0.002	0.208 ± 0.002	1.33 ± 0.15	1.42 ± 0.16
10,0.1,1,2	9.87 ± 0.04	9.21 ± 0.04	0.102 ± 0.001	0.107 ± 0.001	1.54 ± 0.14	2.10 ± 0.18
1,0.1,1,2	0.94 ± 0.02	0.87 ± 0.02	0.107 ± 0.002	0.115 ± 0.002	1.24 ± 0.06	1.33 ± 0.07
10,0.05,1,2	9.58 ± 0.10	7.82 ± 0.05	0.052 ± 0.001	0.061 ± 0.001	1.51 ± 0.20	2.04 ± 0.25
1,0.05,1,2	0.82 ± 0.02	0.69 ± 0.01	0.062 ± 0.002	0.072 ± 0.002	1.22 ± 0.12	1.28 ± 0.12
10,0.02,1,2	8.56 ± 0.19	4.98 ± 0.04	0.024 ± 0.001	0.035 ± 0.001	1.27 ± 0.16	1.42 ± 0.18
1,0.02,1,2	0.48 ± 0.04	0.36 ± 0.02	0.044 ± 0.003	0.055 ± 0.003	1.07 ± 0.08	1.09 ± 0.08
H γ = 0.5 ns; FWHM = 1.7 ns						
10,0.1,1,2	9.86 ± 0.09	9.21 ± 0.07	0.102 ± 0.001	0.107 ± 0.001	1.17 ± 0.09	1.28 ± 0.08
1,0.02,1,2	0.54 ± 0.11	0.36 ± 0.05	0.039 ± 0.008	0.049 ± 0.008	1.09 ± 0.12	1.09 ± 0.12
I γ = 0.1; FWHM = 0.35 ns						
10,0.1,1,2	9.94 ± 0.04	9.28 ± 0.03	0.101 ± ¶	0.107 ± ¶	2.34 ± 0.27	3.78 ± 0.38
1,0.02,1,2	0.52 ± 0.03	0.37 ± 0.01	0.040 ± 0.003	0.052 ± 0.003	1.26 ± 0.15	2.00 ± 0.08

*Average and standard deviation of ten values.
‡τ_1 and τ_2 are in nanoseconds.
¶Standard deviation is <0.0005.

TABLE IV
RESULTS OF ANALYSIS BY METHODS I AND II OF DATA SIMULATED USING
$R(t) = W(t^2e^{-t/\gamma} + 10^{-3}te^{-t/\epsilon})$

	(A_1/A_2)*		τ_1*		CHISQ*	
	I	II	I	II	I	II
J γ = 0.25 ns; ϵ = 1 ns; FWHM = 0.85 ns						
10,0.2,1,2	9.96 ± 0.03	9.80 ± 0.03	0.201 ± 0.001	0.204 ± 0.001	1.37 ± 0.08	1.60 ± 0.11
1,0.2,1,2	0.98 ± 0.01	0.96 ± 0.01	0.205 ± 0.002	0.209 ± 0.002	1.23 ± 0.14	1.29 ± 0.14
10,0.1,1,2	9.86 ± 0.04	9.21 ± 0.04	0.102 ± §	0.108 ± 0.001	1.42 ± 0.14	1.80 ± 0.17
1,0.1,1,2	0.95 ± 0.03	0.88 ± 0.02	0.107 ± 0.003	0.114 ± 0.003	1.19 ± 0.09	1.25 ± 0.10
10,0.05,1,2	9.54 ± 0.10	7.80 ± 0.06	0.053 ± 0.001	0.062 ± 0.001	1.41 ± 0.11	1.76 ± 0.11
1,0.05,1,2	0.83 ± 0.03	0.69 ± 0.02	0.061 ± 0.003	0.071 ± 0.002	1.18 ± 0.10	1.22 ± 0.10
10,0.02,1,2	8.47 ± 0.36	4.96 ± 0.09	0.024 ± 0.001	0.035 ± 0.001	1.22 ± 0.09	1.31 ± 0.09
1,0.02,1,2	0.53 ± 0.05	0.38 ± 0.03	0.040 ± 0.004	0.051 ± 0.004	1.14 ± 0.16	1.15 ± 0.11
K γ = 0.65 ns; ϵ = 1 ns; FWHM = 2.2 ns						
10,0.1,1,2	9.93 ± 0.06	9.28 ± 0.04	0.101 ± 0.001	0.106 ± 0.001	1.06 ± 0.10	1.12 ± 0.11
1,0.02,1,2	0.57 ± 0.17	0.39 ± 0.07	0.040 ± 0.016	0.050 ± 0.015	1.06 ± 0.11	1.06 ± 0.11
L γ = 0.25 ns; ϵ = 1 ns; FWHM = 0.85 ns						
10,0.1,1,2	9.90 ± 0.17	9.26 ± 0.14	0.101 ± 0.002	0.106 ± 0.002	1.08 ± 0.09	1.10 ± 0.09
1,0.1,1,2	0.57 ± 0.18	0.39 ± 0.09	0.038 ± 0.014	0.046 ± 0.015	1.06 ± 0.09	1.06 ± 0.09

*Average and standard deviation of ten values.
†τ_1 and τ_2 are in nanoseconds.
‡Standard deviation is <0.0005.

and τ_1 obtained by the method I are in good agreement with the expected values, whereas the performance of method II is far from satisfactory. In the case of $(A_1, \tau_1, A_2, \tau_2) = (1, 0.02, 1, 2)$ method I has not been successful in producing the expected values. The performance of method II is, however, worse. Similar poor performances of method I were observed for $A_1 = 1$ and $\tau_1 = 0.02$ in the case of other excitation functions B–L. This indicates that the precision in the short-time data is not sufficient for a satisfactory decay data analysis.

The results of analysis of data simulated for excitation functions B to L are given either fully or partially in Tables I to IV. These results confirm that method I is consistently better than method II in producing the optimised values of (A_1/A_2) and τ_1 closer to the expected values with a lower value for CHISQ.

In the calculation of excitation data R_i in 50 ps interval using Eqs. (11)–(14) one can choose the values for parameters (say, γ in Eq. [13]) such that the peak of the chosen function is or is not a data in R_i. For example, in the case Eq. (13) the peak of $R(t)$ occurs at $t_m = 2\gamma$ and the peak is included in the excitation data for all the simulations using functions *G*, *H*, and *I* (Table III). The effect of varying the peak position (t_m) on the results of emission data analysis was also examined. γ in Eq. (13) was varied from 0.18 to 0.22 ns so that the peak occurs between 360 and 440 ps. Excitation and emission data (for $A_1 = 10$, $\tau_1 = 0.1$ ns, $A_2 = 1$ and $\tau_2 = 2$ ns) were calculated in the interval of 50 ps. In these simulations the peak of $R(t)$ is not a data in R_i except in the case when $\gamma = 0.2$ ns. The results of the data analysis of 10 sets of simulation data for each value of γ are shown in Fig. 1. It is observed that the performances of methods I and II are independent of the actual peak position of the analytic excitation function and that method I is consistently better.

It is generally accepted that a large peak count in the fluorescence decay data improves the precision in the values of the lifetimes in a multiexponential fitting. This is achieved because the signal to noise ratio increases as $N^{1/2}$ in photon counting experiments, N being the number of counts. The performances of both the methods were compared at various levels of signal to noise ratio in the fluorescence decay data which were simulated by varying

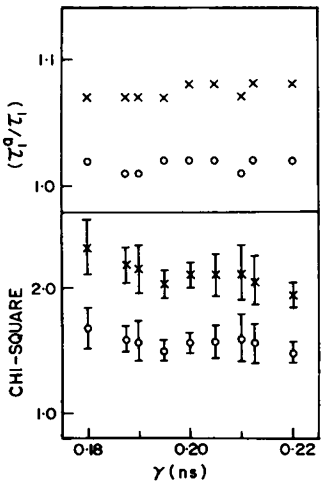

FIGURE 1. Plot of optimised values (average of ten) of the short lifetime (τ_1^a/τ_1, *top*) and chi-square (*bottom*) obtained in the analysis of data by method I (o) and by method II (x) versus γ. See text for details.

W using excitation function A. The following values were used for the parameters in Eq. (15): $A_1 = 10.0$, $\tau_1 = 0.1$ ns, $A_2 = 1.0$, and $\tau_2 = 2.0$ ns. Ten sets of excitation and emission data were simulated for each W. Deconvolution analysis by method I produced consistently better results (i.e., A_1/A_2, and τ_1 were closer to the values used in simulation) compared with method II for all W; however, for $W < 1 \times 10^4$, the analysis by both the methods gave chi-square values which are nearly equal. Fig. 2 shows the variation of the chi-square values obtained in the analysis by method I and II as a function of W. The data analysis by either method gave a chi-square value which increased with increasing W, the increase being steeper in the case of method II. This indicates that the numerical integration proposed here is better than the trapezoidal approximation for handling precision data.

Methods I and II were then compared with the analysis of data simulated for various values of the short lifetime component. The simulation parameters were as follows: $W = 10^5$, $A_2 = 1.0$, $\tau_2 = 2.0$ ns, and $A_1 = 10.0$. τ_1 was varied from 0.02 to 1.0 ns. For each value of τ_1 ten sets of excitation and emission data were simulated. These simulation data were analysed and Fig. 3 *A* shows the variation of the chi-square values obtained by both the methods. Fig. 3 *B* shows the ratio (τ_1^a/τ_1) obtained by both the methods, τ_1^a being the average of ten optimised values of τ_1 obtained in the analysis. It is found that method I is able to extract the short lifetime component more correctly and with better values for statistical test parameters. However, for $\tau_1 > 0.5$ ns both the methods are equally efficient.

The randomness of the distribution of weighted residuals is usually checked by the calculation of reduced chi-square and other test parameters. It is instructive to examine also visually the distribution of the weighted

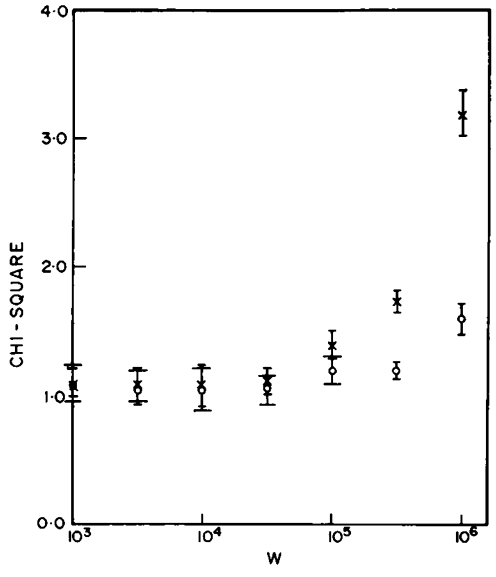

FIGURE 2. Variation of the values of chi-square obtained by method I (o) by method II (x) for various values of W. See text for details.

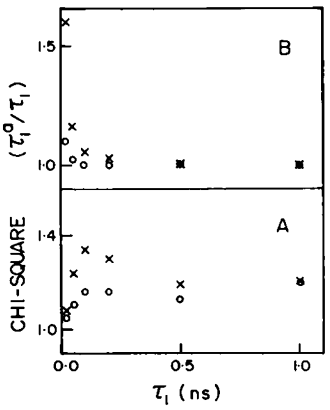

FIGURE 3. Plot of optimised values (average of ten) of the short lifetimes (τ_1^a) (plotted as τ_1^a/τ_1, *top*) and chi-square (*bottom*) obtained in the analysis of data by method I (o) and by method II (x) versus τ_1. δt = 50 ps for all simulated data. See text for details.

residuals. Fig. 4 shows a typical display of the weighted residuals obtained by methods I and II in the analysis of simulation data using Eq. (11) for excitation function ($\sigma = 0.2$ ns, $m = 1.2$ ns, and $W = 1 \times 10^5$), and Eq. (15) for $I(t)$ ($A_1 = 10.0$, $\tau_1 = 0.1$ ns, $A_2 = 1$, and $\tau_2 = 2$ ns). The simulated excitation data, emission data, and fitted emission data (method I) are shown in Fig. 4. In this case the emission data was not normalized and the peak count was $\sim 1.2 \times 10^5$. The distribution of the weighted residuals in the region dominated by the short lifetime component is more acceptable in Fig. 4 *B* than in Fig. 4 *C*. Deconvolution by method I produced the following results: $A_1 = 10.0$, $\tau_1 = 0.101$ ns, $A_2 = 1.01$, $\tau_2 = 2.00$ ns, (reduced) chi-square = 1.17, Durbin-Watson parameter (DWP) = 1.90, standard normal variate of runs test (Z) = -0.05, and percentage of weighted residuals between -2 and $+2$ (PER) = 95.09. Deconvolution by method II produced the following results: $A_1 = 9.44$, $\tau_1 = 0.106$ ns, $A_2 = 1.01$, $\tau_2 = 2.00$ ns, chi-square = 1.41, DWP = 1.59, Z = 1.58, and PER = 92.77.

In the simulations described earlier the time interval was chosen to be 50 ps. The conclusion that the performance of method I is better than method II when the short lifetime in the decay equation is comparable to δt is independent of the value of δt used in simulations. The computation time required for method I or method II depends upon the number of iterations required for convergence, which need not be equal. On the average it is observed that method I requires ~10% more computer CPU time (Cyber 170/730) than that required for method II. However, there were several cases in which method I required less time than method II because of convergence at a lower interation number.

The method proposed here has also been used in the analysis of experimental fluorescence data of standard samples obtained by time-correlated single photon counting technique. In comparison with the simulation data the quality of the experimental data was poor because of system errors, especially the wavelength response of the photomultiplier which needed to be corrected in the analysis by introducing a shift parameter. In spite of this, it is generally observed that method I generates results with

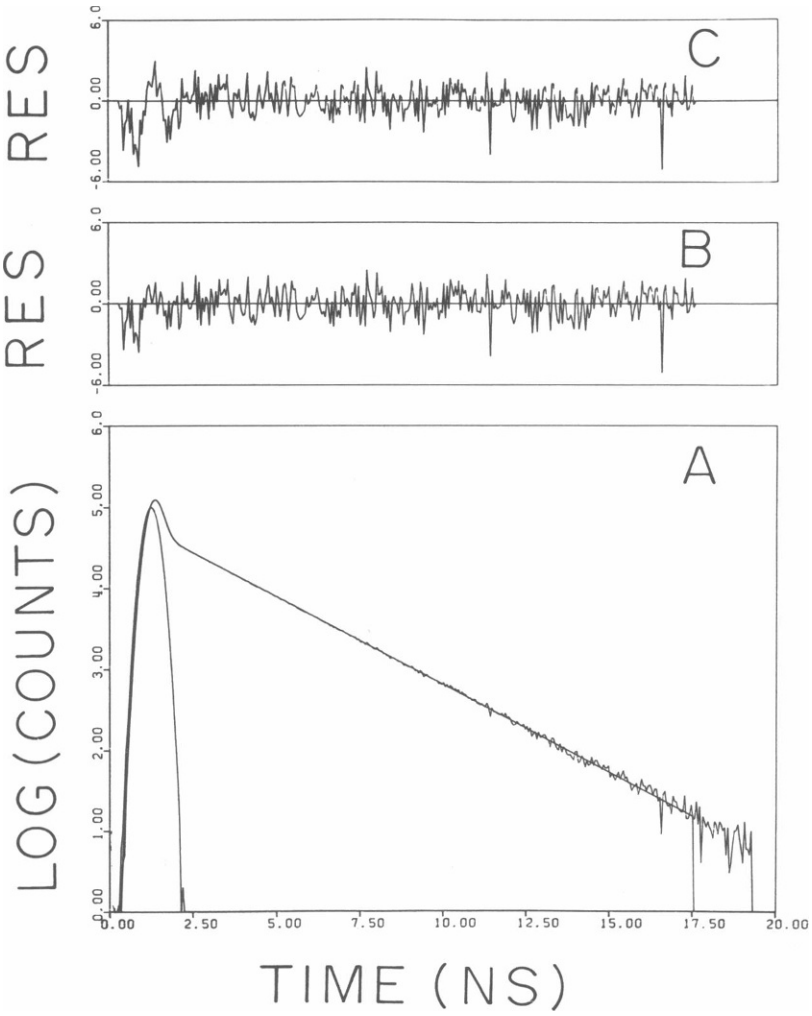

FIGURE 4. (*A*) Gaussian excitation curve, simulated fluorescence decay curve for a two exponential decay equation, and the smooth fluorescence decay curve obtained in fitting the emission data by method I. See text for details. (*B*) Distribution of weighted residuals obtained by method I and (*C*) by method II.

statistical test parameters that are marginally better than those obtained by method II. It is not uncommon in the analysis of experimental data to encounter a distribution of residuals which appears bad only in the peak region in a multiexponential fit of fluorescence decay. When all instrument related errors are eliminated as a source of this discrepancy, we suggest that one must also examine other approximations for the numerical computation of Eq. (1).

CONCLUSION

In conclusion, use of recursion relations (Eqs. [5], [7], and [8] is recommended in the deconvolution analysis of fluorescence decay data by the nonlinear least-squares method when a short lifetime component is suspected.

The author would like to thank Professor B. Venkataraman for a critical reading of the manuscript.

Received for publication 10 March 1988 and in final form 31 May 1988.

REFERENCES

1. Bevington, P. R. 1960. *In* Data Reduction and Error Analysis for the Physical Sciences. McGraw-Hill, Inc., New York.
2. Yguerabide, J., and E. Yguerabide, 1984. *In* Optical Techniques in Biological Research. D. L. Rousseou, editor. Academic Press Inc., Orlando, FLA. 206–213
3. Grinvald, A., and I. Z. Steinberg. 1974. On the analysis of fluorescence decay kinetics by the method of least-squares. *Anal. Biochem.* 59: 583–598.
4. O'Connor, D. V., and D. Phillips. 1984. *In* Time-Correlated Single Photon Counting, Academic Press, Inc., London. 175.
5. Demas, J. N. 1983. *In* Excited State Lifetime Measurements. Academic Press, Inc., New York. 209.
6. Van den Zegel, N. Boens, D. Daems, and F. C. De Schryver. 1986. Possibilities and Limitations of the Time-Correlated Single Photon Counting Technique: A comparative study of correction methods for the wavelength dependence of the Instrument Response Function. *Chem. Phys.* 101:311–335.